Journal Pre-proofs

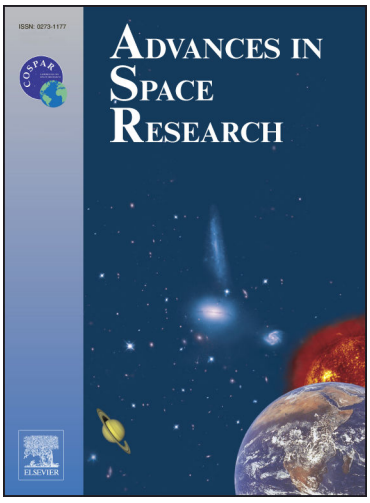

Can the Comprehensive Model (CM4) predict global features of sudden commencements?

Adel Fathy, Richard Holme

PII: S0273-1177(20)30412-9
DOI: https://doi.org/10.1016/j.asr.2020.06.010
Reference: JASR 14833

To appear in: *Advances in Space Research*

Received Date: 7 August 2019
Revised Date: 6 June 2020
Accepted Date: 10 June 2020

Please cite this article as: Fathy, A., Holme, R., Can the Comprehensive Model (CM4) predict global features of sudden commencements?, *Advances in Space Research* (2020), doi: https://doi.org/10.1016/j.asr.2020.06.010

Title

Can the Comprehensive Model (CM4) predict global features of sudden commencements?

Adel Fathy[1], Richard Holme[2]

1-Physics Department, Faculty of Science, Fayoum University, Egypt.

e-mail: afa05@fayoum.edu.eg

2-School of Environmental Sciences, University of Liverpool, UK.

e-mail: R.T.Holme@liverpool.ac.uk

Abstract

We investigate the capability of the Comprehensive model CM4 to predict features of geomagnetic sudden commencements (SCs) focusing on observations from five ground-based observatories along the African chain. A list of 153 SC events has been selected within the period 2011 to 2015 to compare between modelled and observed SCs at different seasons and local times. The study reflects the degree of consistency between the CM4 model and the real physics occurring at each ground station. It also compares the characteristics of observed and modelled SC field to show how well the model performs for predicting the SC field variation. Results of feeding the CM4 model by the SYMH index data shows that the CM4 model provides a reasonable fit of the observed SC field at stations located closer to the average latitude of Dst index stations. Positive SC field variations during the day and night times for both CM4 modelled and observed fields are expected to be a signature of the magnetopause and field aligned currents rather than the axial ring current. The dawn-dusk asymmetry of the SC modelled field, which resembles the observed field at stations located poleward of the equatorial region, reveals a significant contribution from the partial ring current. At the magnetic equator, the equatorial ionospheric electrojet current plays a significant role in enhancing the observed SC field during daytime hours, which is not parameterized in the CM4 model. The latitudinal profile of the modelled field exhibits its maximum variation at the magnetic equator, decreasing towards the poles. This latitudinal profile resembles the observed field but is weaker. The modelled field at the latitudes of the Dst index stations has the same local time features of the observed field, but its strength is much smaller than the observed field and also it does not exceed its corresponding SYMH variations. In addition, the modelled SC field has a weak smooth variation with respect to local time, unlike the broad scattering of the observed field. Despite the substantial correlation between the modelled SC field and its associated SYMH field variations, the model always under-estimates the SYMH variations even at the magnetic equatorial station. Also, the CM4 model has no information about the SC seasonal variation, even at stations located within the same latitudes of the Dst index stations. These limitations should be considered when using the CM4 model to describe the external magnetospheric field.

Keywords: CM4; magnetosphere; sudden commencement

Introduction

The Inter-Planetary (IP) shock compresses the day side Earth's magnetic field and causes a step like increase in the horizontal magnetic field (H-component) which is known as a Sudden Commencement (SC). The main cause of SCs is the sudden increase of the magnetopause current （Chapman-Ferraro Current : CFC) due to the dynamic pressure increase associated with the IP shock. The step-like increase of the H-component is produced at low latitude stations by the magnetospheric compression transmitted by the fast mode HM waves. At high latitudes, a bipolar variation appears which is interpreted in terms of Field Aligned Currents (FACs) and FAC-generatedIonospheric Currents (ICs) (Araki 1994). The strength of SCs decreases with increasing latitude but increases again toward high latitudes. It is strongly enhanced along the dayside dip equator (Araki 1994; Shinbori et al., 2004; Shinbori et al., 2009).

The criterion for selecting SCs has been defined as a sudden increase of 5 nT within 10 minutes in the SYMH index (Fathy et al., 2018; Park et al., 2014; Park et al., 2012; Shinbori et al., 2009). Therefore, the signatures of SCs in the SYMH index are similar to that observed in the horizontal magnetic field component at low and mid-latitudinal stations. Both SYMH and Dst indices are not a pure representation of the Ring Current (RC), but have contributions of large scale magnetospheric currents such as the CFC, RC, FACs, and Tail Currents (TC). Li et al. (2011) showed that the dominant contribution of the partial RC to the main phase H component of moderate geomagnetic storms disappears during super storms because of its saturation. Burton et al. (1975) introduced a correction to remove the contribution of the CFC from the Dst index, defining the pressure-corrected Dst index Dst^* (Rawat et al., 2010 and references therein). Kalegaeve et al. (2005) showed that the contribution of the TC and RC are comparable during moderate magnetospheric storms, while RC becomes dominant during an intense magnetic storm; this result supports those of Turner et al (2000) who showed that the TC has a contribution of ~25% in the presence or absence of substorm. Kalgaeve and Makarenkove, (2008) studied the contribution of the TC and the RC to the Dst index. Kalgaeve concluded that the TC has a comparable contribution with the RC during moderate storms while the RC dominates during strong ones. Further, the substorm current wedge and Earth induction currents which are produced due to differences in conductivity around each station also contribute (Mcpherron et al., 1999). The FACs have been suggested to be the main cause of night-time positive magnetic enhancements during

SCs at middle, low and equatorial latitudinal regions (Araki et al., 2006 and Shinbori et al., 2009).

This complex set of contributions of several magnetospheric currents to the Dst/SYMH index is directly reflected within the CM4 model because it relies on the Dst index to predict the effect of external magnetospheric currents. Therefore, SCs observed in the SYMH index can be modelled using the CM4 model. Although the CM4 model is constructed to fit the magnetic field during solar quiet periods, Sabaka et al., (2004) identified that the Dst index has an approximate linear relationship at low latitude to storm time activity in the horizontal component up to 200-300 nT; therefore, the Dst index may still represent the physics of the external magnetic field during active conditions. Onovughe and Holme (2015) and Onovughe (2016) showed that the CM4 produces more reasonable predicted than expected under moderately active conditions $Kp \leq 5$ for predicting the diurnal variations of long wavelengths. Onovughe attributed misfit between the observed and predicted data to the existence of short time variations in the observed data, too rapid to be reflected by the Dst index. So, adapting the CM4 model by updating its inputs with the high tim e resolution SYMH index rather than the Dst index could reduce the misfit and also extract short time variations like SCs. Note that although CM4 is defined up until 2002.5, this limit applies only to the internal field, and so we can use the model here to investigate the magnetospheric field at more recent times.,

This work investigates the CM4 model prediction of the geomagnetic SCs at 5 ground based stations separated in latitude along the African chain and studies its local time (LT) and seasonal dependence, comparing the observed ground SCs with the modelled SCs of the CM4 model. We investigate the extent to which the SC data can be fit by this model. This will give insight into the mechanisms that lead to the phenomenon and might also lead to some predictive capability.

The Comprehensive Model (CM4)

The Comprehensive Model (CM4) is a global model initiated by Sabaka and Baldwin (1993) to parameterise the near Earth's magnetic field by its individual sources (core, lithospheric, ionospheric, magnetospheric and induced fields). It uses quiet time data, both vector and scalar, from ground-based observatories and satellite (MAGSAT, POGO, ORSTED and CHAMP) measurements to resolve parameterization between internal,

ionospheric and magnetospheric sources (Sabaka et al., 2002). The ability to model various source fields simultaneously overcomes the problem of frequency overlapping between the spectra of various source fields that arose in other models which isolated only a single-source field; external fields are parameterized using the Dst magnetic index and the F10.7 solar flux index. Ground-based data has been selected around midnight during the quietest days. The space data has been selected for quiet conditions, where Dst index values are within $\pm 20\, nT$ and the Kp $\leq 1^o$ or $\leq 1^+$ and also $\leq 2^o$for the previous three hours. CM4 is not expected to give good results away from these conditions. To minimize the effect of the FACs and ionospheric currents in the auroral regions, only scalar satellite magnetic field data poleward of $\pm 50^o$ magnetic latitude are included. Fields due to RC and solar flux are restricted to external magnetospheric and ionospheric fields respectively. External magnetospheric field in the CM4 model is parameterized by the Dst index, containing signals with periods that vary from hours to a few days during quiet days (Sabaka et al., 2002 and 2004). The relevant CM4 external harmonic coefficients of the magnetospheric contributions are parameterized to vary linearly with Dst index (Langel and Estes, 1985a). The model adopted only dipole terms (harmonic n = 1) to describe large-scale external magnetospheric fields that may have a signal arising from the Dst index. The model modulates the temporal variability of $D_{st}(t)$ index by both regular daily and seasonal periodicities to describe the local time (LT) variability/asymmetry.

Data set and event selection

The high time resolution (1 minute) SYMH index data was obtained from OMNI website ftp://spdf.gsfc.nasa.gov/pub/data/omni/omni_cdaweb/hro_1min/ and was visually inspected to look for SCs. SCs criterion is defined as a sudden increase of 5 nT within 10 minutes in the SYMH index (Fathy et al., 2018; Park et al., 2014; Park et al., 2012; Shinbori et al., 2009). A list of 153 SC events observed from 2011 to 2015 has been selected according to this criterion. The onset time of the SC event is defined as the time at beginning of the sudden increase in the SYMH index and the saturation time is defined as the time at the first local maximum after the onset time. The difference between the saturation and the onset times of the SYMH index is denoted by $\Delta SYMH$ in the current work. The rise time is defined as the time difference between the onset and saturation times.

Figures 1a-b present a typical example of an SC event, observed on April 6, 2011 at AAE observatory, and its appearance in the SYMH index. Red circles illustrate the location of the

SC onset and saturation times. At AAE station, the onset and saturation times are at 09:34 and 09:37 UT respectively, while the onset and saturation times of the SYMH index are at 09:35 and 09:39 UT respectively, giving a rise time of 4 minutes. Because the onset and saturation times of ground stations differ from those of the SYMH index, the onset and saturation times of each SC event were separately determined at each of the 5 stations used. The difference in the field between the onset and saturation time at AAE station is $\Delta B_X = 59\,nT$ as shown in Fig. 1a, while the difference of the field between the onset and saturation time of the SYMH index is $\Delta SYMH = 25\,nT$ as shown in Fig. 1b. Since the SYMH index is derived in the same way as the Dst index, feeding the CM4 model with the high time resolution SYMH index data rather than the hourly Dst index data enables us to investigate the features of rapid geomagnetic phenomenon like SCs.

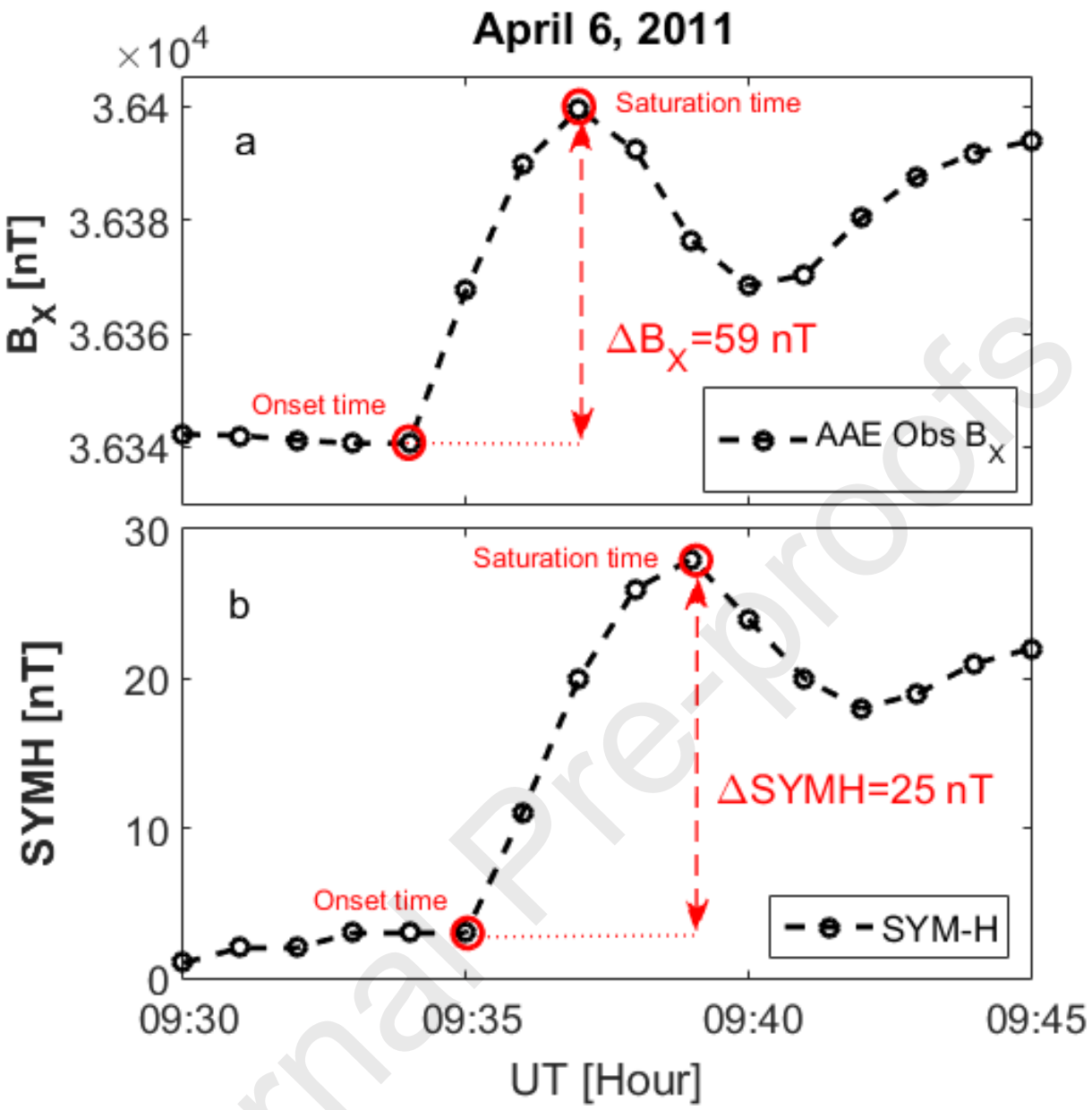

Fig. 1 a) A typical SC example observed on April 6, 2011 at AAE station. Red circles illustrate the location of the onset and the saturation times and the vertical red double arrow represents the SC field variation ΔB_X, b) the same SC event variation but in the $SYMH$ index.

Figures 2a-c illustrate the magnetospheric conditions associated with the same event: the Kp index (a), the Auroral Electrojet (EEJ) indices (AL and AU) in nT (b), and the SYMH index in nT (c). Fig. 2 shows that the AL index did not decrease to less than 100 nT and the SYMH index increased from 3 nT at the onset time to 27 nT at the saturation time. The values of the SYMH index at the onset and the saturation times are still close to the limits under which the CM4 model derived, but the Kp = 5, far from the $Kp < 1^0$ CM4 criterion implies moderately disturbed magnetospheric conditions.

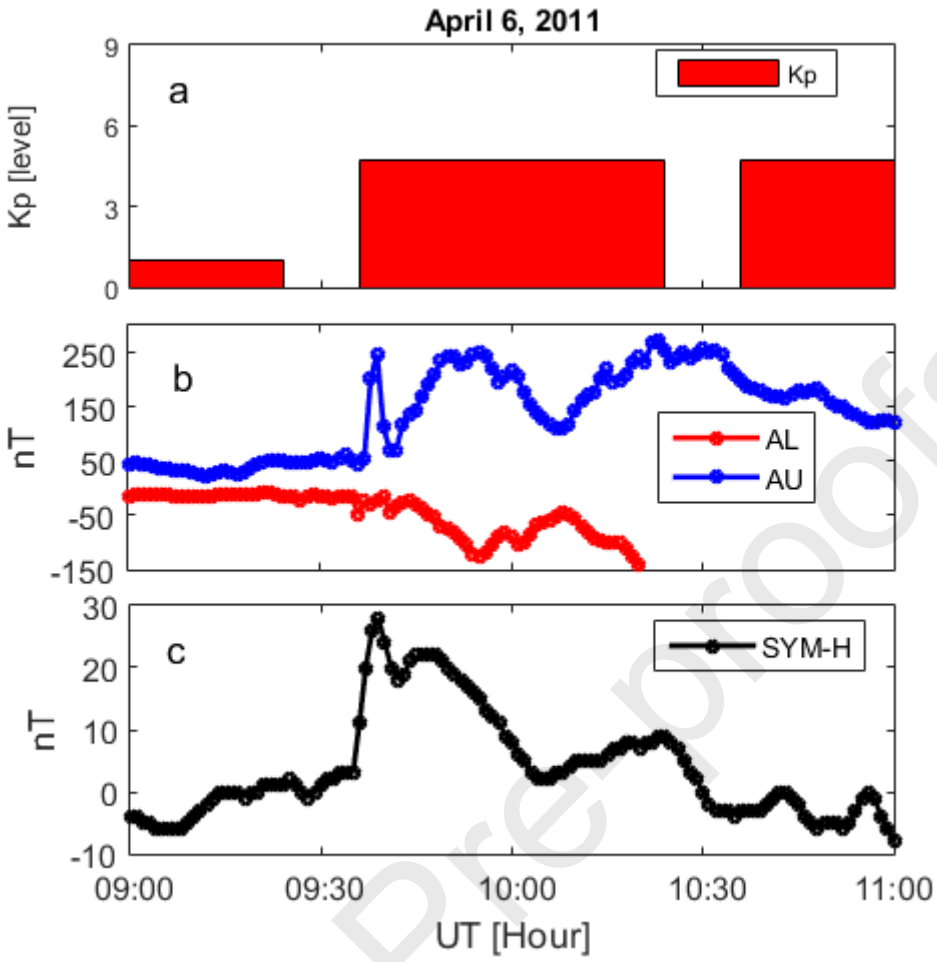

Fig. 2 Geomagnetic conditions associated to SC event observed on April 6, 2011, a) Kp index(level) value times 10, b) Auroral electroject indices AL and AU and c) SYMH index.

The five stations (PEG, TAM, AAE, TSU and HER) from which ground based magnetic field data were obtained belong to the INTERMAGNET network of observatories (http://www.intermagnet.org/index-eng.php). The geographic and geomagnetic locations of these stations are listed in table 1.

Code	Name	Geographic		Geomagnetic	
		Colatitude	Longitude	Latitude	Longitude
PEG	Pedeli	51.9	23.9	36.36	103.36
TAM	Tamanrasset	67.21	5.53	24.79	81.59
AAE	Addis Ababa	80.97	38.77	5.22	111.43
TSU	Tsuemb	109.20	17.58	-18.67	85.31
HER	Hermanus	124.4	19.23	-33.84	83.37

Table 1. The geographic and geomagnetic coordinates of the 5 INTERMAGNET geomagnetic observatories used in the current study.

Figure 3 illustrates the geographic location of ground observatories. Stations are ordered in table 1 according to latitudinal location from the north to the south hemisphere to give some sense of separation distance from the equator in both hemispheres. Stations have been selected to be as close as possible in longitude and also separated in latitude to show the behavior of ΔB_X associated to SCs with distance from the magnetic equator. . The red solid line illustrates the location of the geomagnetic dip equator. We chose stations along the African chain because HER geomagnetic observatory belongs to the 4 ground based stations used for deriving the Dst index, so t its observed SC field variations (ΔB_X) are expected to resemble the modelled CM4 SC field. For abbreviation, the variation of the observed magnetic field in the horizontal X components associated to SC is denoted by ΔB_X, while the modelled field using the CM4 model is denoted by the CM4 ΔB_X.

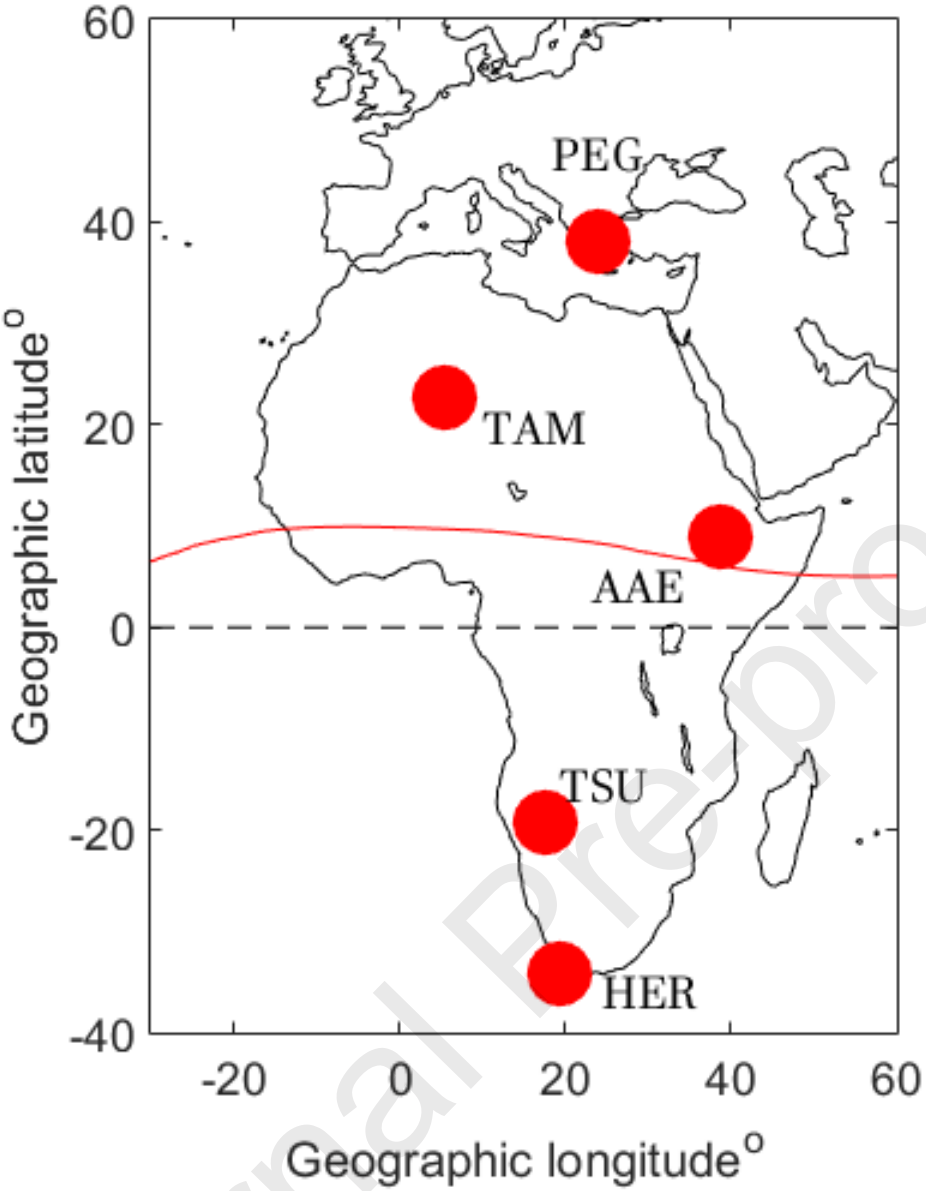

Fig. 3 The geographic latitude and longitude of the 5 INTERMAGNET ground based observatories in red dots, the red solid line illustrates the geomagnetic dip equator. The dashed black line is the geographic equator.

The CM4 prediction of the magnetic field at a ground station depends on input parameters of the colatitude and longitude of the station, the universal time of the measurement, and the corresponding value of the SYMH index. The difference of the modelled field between the onset and the saturation time is defined as the CM4 ΔB_X. This is then normalized by the by the strength of the SC event given by the $\Delta SYMH$ field - $\frac{CM4\ \Delta B_X}{\Delta SYMH}$ to overcome the variability of the solar wind strength from one event to another, enabling investigation of the SC seasonal and the local time dependence

Figure 4 shows for SC event on April 6, 2011 the profiles of the observed geomagnetic field B_X and its corresponding modelled CM4 B_X field as functions of local time in blue and red lines respectively. Stations are ordered from top to bottom by latitude from north to south. A constant offset between the modelled and observed fields has been subtracted arising from unmodelled short wavelength crustal field. The offset value for each station is defined as the average of the difference between the observed and modelled field within midnight hours during the 5 quietest days. After elimination of this offset, CM4 closely resembles the observed field as shown by Fig. 4. The left column illustrates the observed and the modelled field over the whole day (24 hours), while the right column focuses on the time of the SC event from 09:30 to 09:45 UT. The change of the field in shown in the right column is calculated as difference between the field and mean value of 3 minutes before the onset time. Fig. 4 shows that at the SC onset time 09:33 UT, the modelled field increases in a similar manner to the observed field. Both observed and modelled CM4 fields at stations away from the magnetic equator have the same smooth variation in, while the equatorial station AAE has a dramatic enhancement in the observed field in comparison to the modelled field. The positive enhancement during the SC event at ~12:00 LT is expected to be due to the CFC and not the axial RC, because RC would show a negative signature at stations located away from the equator. As explained above, because the CM4 is parameterized by the Dst index, with contributions from /the CFC, PRC, TC, FAC and RC, these positive enhancements associated to SCs are also to expected in the model prediction.

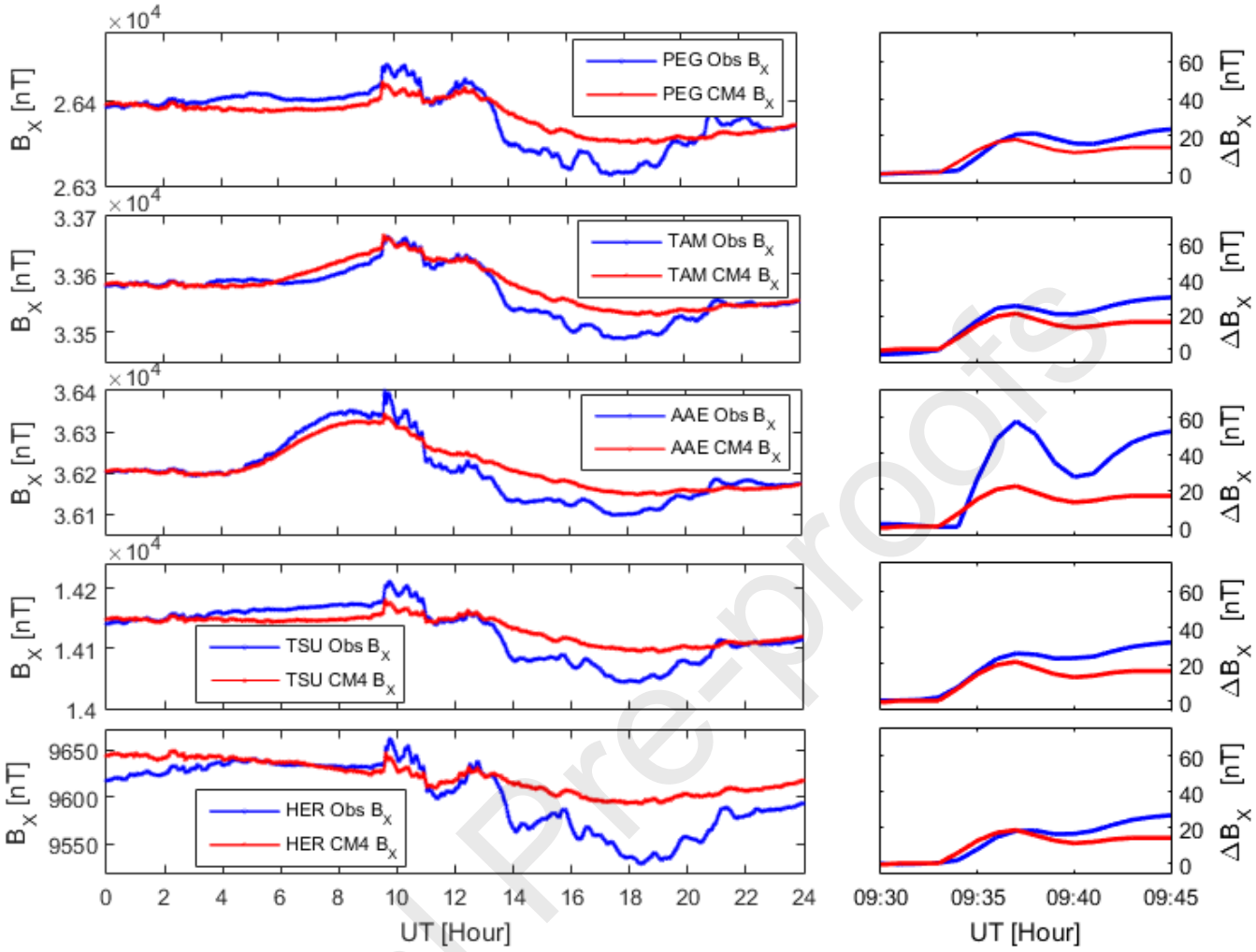

Fig. 4 Left column shows a profile of the observed B_X field and its corresponding modelled field using the CM4 in blue and red colors respectively on April 6, 2011. Right column zooms in around the appearance time of the SC event. Stations ordered from top to bottom by latitude (table 1).

Statistical Results

Values of geomagnetic indices presented in Fig. 2 show that for this event the magnetosphere was not strongly disturbed: SYMH index values at both the onset and saturation times are close to the derivation limits of CM4 ($\pm 20\ nT$)., suggesting that CM4 predictions can be useful. However, it is necessary to investigate the values of the SYMH and Kp indices for the complete SC events presented in the current study to provide a full description of the magnetospheric conditions under which the SC has occurred. The mean

value of the Kp index during the onset time for each geomagnetic SC event is shown in Fig. 5a. The dashed red line in Fig. 5a represents the Kp value at level 5. The auroral electrojet indices AL and AU values in nT at the onset time are shown in Fig. 5b in black and blue solid circles respectively, and the SYMH values at the onset and saturation times are shown in Fig. 5c as black solid and blue open circles respectively, while the horizontal red dashed lines at $SYMH = \pm 20\ nT$ represent the limits of the Dst index used in deriving CM4. Fig. 5a shows that the majority of SC events in the period 2011-2015 are observed at times of no more than moderate level activity ($\mathrm{Kp} \leq 5$) as indicated by the red dashed line. Also, the majority of SYMH index values during the onset time are within the confidence limits of the Dst index in the CM4 model as shown by horizontal red lines at $\pm 20\ nT$ in Fig. 5c, although at saturation time many SYMH values exceed these limits as indicated by open blue circles.

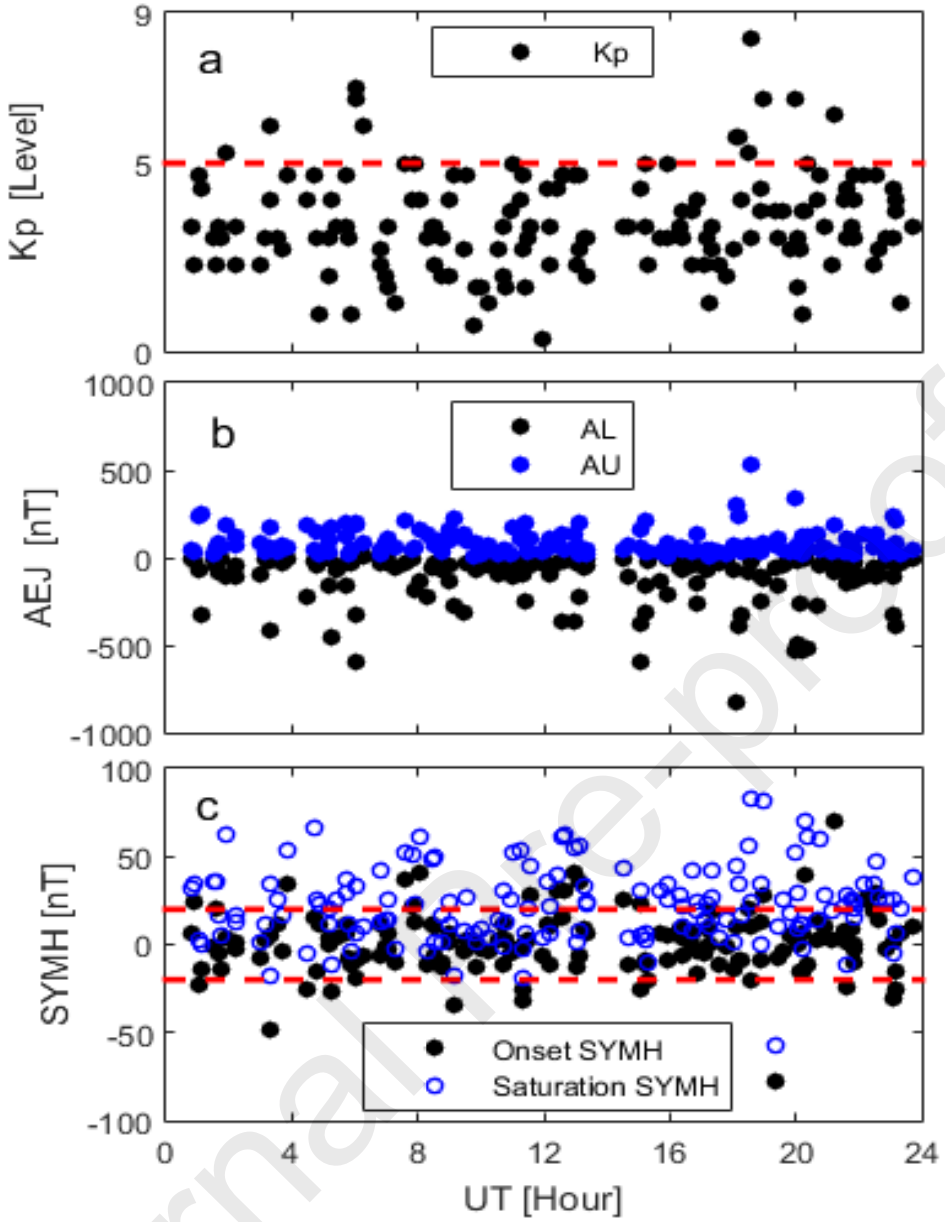

Fig. 5 (a) The Kp index level associated to SCs, b) AL and AU indices values in nT associated to the same onset time of SCs c) the SYMH index values in nT at the onset and saturation times in solid black and open blue circles of SC events.

For each INTERMAGNET station, the relationship between the normalized observed field in the X component $\frac{\Delta B_X}{\Delta SYMH}$ and the local time is shown in the left column of Fig. 6. Red, blue and black open circles in Fig. 6 represent events observed in summer months (June , July and August), winter months (December, January and February) and spring/autumn months (March, April, May, September, October and November) respectively. Green bars give the standard deviations around the median value within each hour. Note the greater range of the

Y-axis scale for the observed field $\frac{\Delta B_X}{\Delta SYMH}$ in the left column compared with the modelled CM4 $\frac{\Delta B_X}{\Delta SYMH}$ field in the right column, highlighting the local time variation of the field, and the difference of the field variations between the observed and the modelled fields. The equatorial station AAE (5.2^o magnetic latitude) shows a maximum magnetic field variation within the pre-noon local time at approximately 10:00 LT. This enhanced pre-noon peak for equatorial stations is known as the equatorial enhancement of the SC peak (Ferraro and Unthank, 1951; Araki 1994). The minimum variation of $\frac{\Delta B_X}{\Delta SYMH}$ at AAE station observed after midnight local time as shown in Fig. 6c.

Values of the normalized field at TAM and TSU geomagnetic observatories located at 24.79^o and -18.67^o magnetic latitudes approach unity ($\frac{\Delta B_X}{\Delta SYMH} \sim 1$) and have non-clear dawn-dusk asymmetry. PEG and HER stations which are located at 36.36^o and -33.84^o magnetic latitudes, have their minimum field variation within the morning at 08:00 LT. PEG station shows a maximum field variation near the dusk time at17:00 LT, while HER station has its maximum field variation within afternoon at 15:00 LT. This dawn-dusk time asymmetry is attributed to the contribution of the PRC (Li et al., 2011). In the northern hemisphere (at PEG station), the summer SC strength is larger in comparison to winter SC field strength, while in the southern hemisphere (at HER station) the summer SC strength is smaller than in winter SC field strength. This seasonal variation appears clearly from 12:00 LT to 24:00 LT. The equatorial station AAE does not show seasonal variation with respect to local time.

The corresponding CM4 modelled field of each station is shown in the right column of Fig. 6. It illustrates the variation of the modelled (CM4 $\frac{\Delta B_X}{\Delta SYMH}$) external magnetospheric field with respect to LT. The modelled ΔB_X field represents the combined (primary and induced) magnetospheric fields associated to the geomagnetic SCs. Generally speaking, the variation of the modelled field with respect to the LT for the 5 stations is similar except in their strength. The modelled field approaches unity (CM4 $\frac{\Delta B_X}{\Delta SYMH} \sim 1$) during afternoon and equals 0.8 in the early morning at the equatorial station (AAE), which resembles the observed field at station located poleward of the magnetic equator Also, no enhanced equatorial anomaly field at AAE station is seen, and no seasonal variations are seen at PEG and HER stations. The summer, winter and spring/autumn seasons are randomly distributed at whole local times, also this random distribution is similar at all stations: the CM4 model has no

information about the seasonal variations of the SCs field. The maximum value of the modelled field does not exceed 1, in other words the maximum CM4 ΔB_X field does not exceed the maximum value of the $\Delta SYMH$. This result is expected, because the CM4 is parameterized over the Dst index.

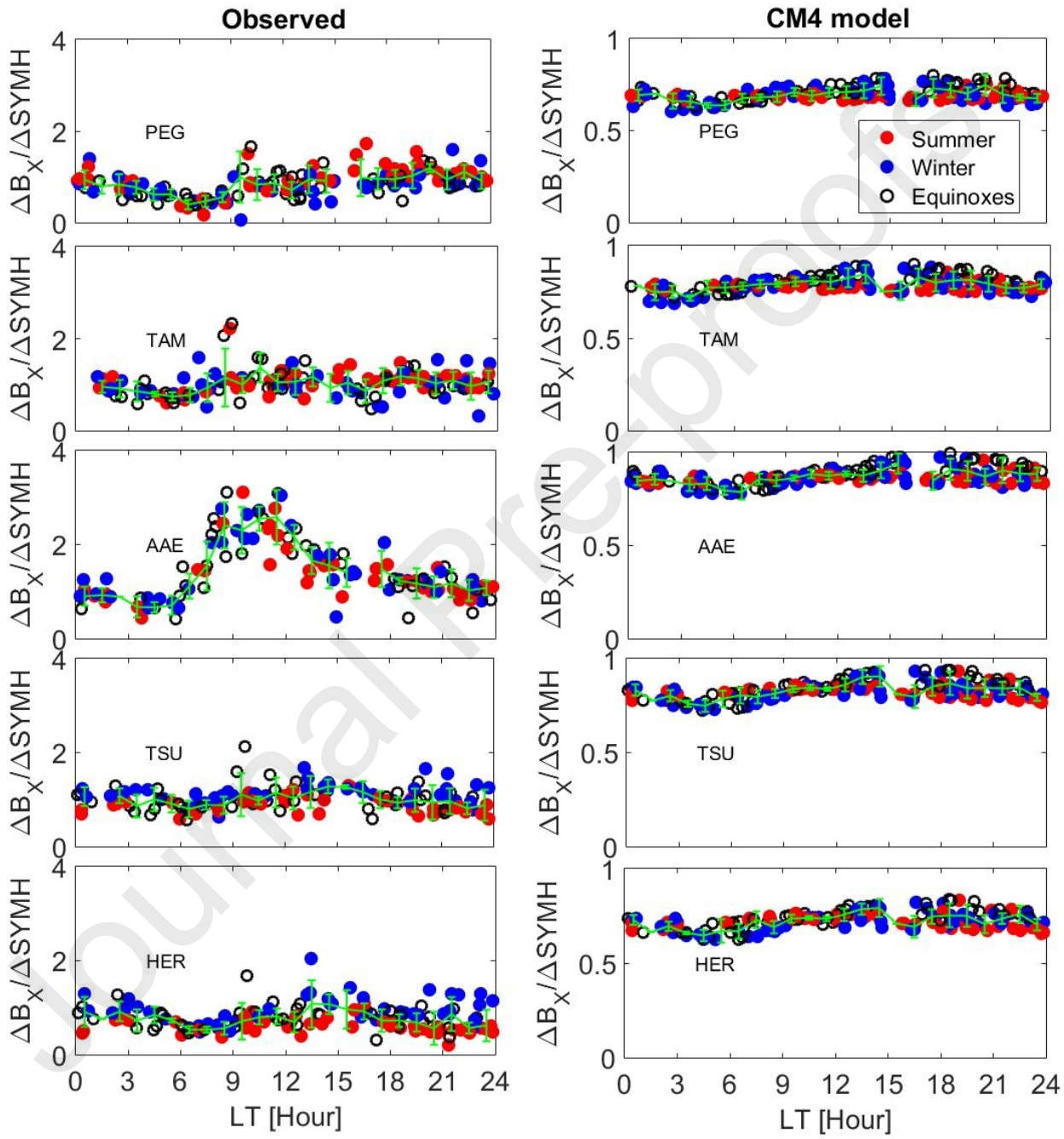

Fig. 6 Variation of the normalized observed field $\frac{\Delta B_X}{\Delta SYMH}$ and the combined modelled magnetospheric field CM4 $\frac{\Delta B_X}{\Delta SYMH}$ associated with SCs in left and right columns respectively.

Blue, red and open black circles correspond to winter, summer and spring/autumn seasons respectively, while green bars represent the hourly standard deviation around the median. Stations ordered from top to bottom according to their orders in table 1.

A comparison between observed ($\frac{\Delta B_X}{\Delta SYMH}$) and modelled (CM4 $\frac{\Delta B_X}{\Delta SYMH}$) fields with respect to the LT in Fig. 6 shows that the pre-noon enhancement at 10:00 LT only appeared in the observed equatorial data of AAE. The observed and modelled field at both PEG and HER stations vary in a similar manner with respect to LT regardless the differences in field strength. Both observed and modelled fields have their maximum variation within the afternoon and their minimum variation during the early morning time. However, the maximum and minimum field variation observed in the afternoon and in the early morning respectively at both HER and PEG is not clearly observed at TAM and TSU. The strengths of the observed field at TAM and TSU are of comparable strength to the modelled field. The variation of modelled field with respect to LT varies in the same sense of the equatorial station, but the strength of the field decreases at higher latitudes. This comparison shows that the local time features of observed field are more complex than the modelled field using the CM4 model.

The latitudinal profile of the normalized SC field of both observed and modelled fields is shown in Fig. 7. Green, red, black and blue solid dotted lines corresponding to the normalized observed SC amplitude within dawn, noon, dusk and night time local times respectively, while the modelled field is represented by dashed lines. Each point represents the median value of the normalized SC field strength for a certain LT at a specific station as indicated by the legend on Fig 7. The large positive enhancement of the SC field at the equatorial station is observed around the noon LT; other local times also have their maximum variation at the equatorial station. For all local times, the strength of the SC field decreases with moving poleward until 40^0 latitude. It approaches 1 at TAM and TSU station during noon, dusk and night LTs. The gradual decrease of the CM4 modelled field strength with moving poleward matches the observed field but at lower amplitude. The observed dawn-time SC field dramatically decreases in comparison to other local times field at latitudinal regions $> 20^0$. In addition, the modelled field at latitudinal regions $< -20^0$ shows that the dawn time SC strength is much smaller than other local times SC field strength. At any specific location the modelled noon, dusk and night time SC fields have a comparable

strength and their strength are always less than 1 even at the equatorial station. The close values of the SC modelled field during noon, dusk and night times resemble the observed field at PEG, TAM and HER stations but with lower magnitude.

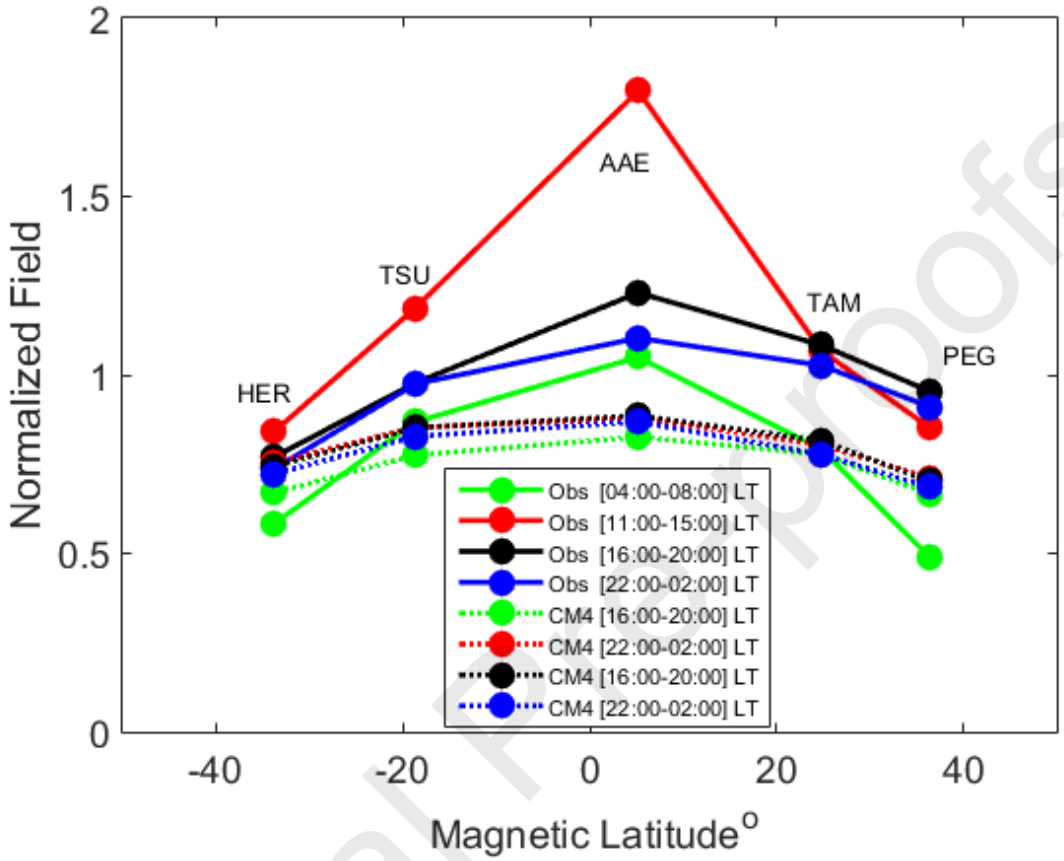

Fig. 7 The latitudinal profile of the normalized SC field strength for both observed and modelled fields in solid and dashed dotted lines respectively. Dawn, noon, dusk and night times corresponding to green, red, black and blue colors respectively.

Fig. 8 illustrates linear fits between the observed field ΔB_X (upper row) and the modelled magnetospheric CM4 ΔB_X (lower row) and the corresponding $\Delta SYMH$ associated with SCs at PEG, TAM, AAE, TSU and HER stations respectively from left to right. Dawn, noon, dusk and night times SC fields are shown in green, red, black and blue respectively. Solid black lines show the linear fitting, with the fitting equation for each station is shown in each panel. Dashed black lines show the prediction of a 1:1 relationship.

Approaching the equator, the gradient of fit increases reaching a maximum of 1.2 at AEE, but simultaneously with minimum correlation coefficient R= 0.74. Moving poleward

the slope decreases and to a minimum at HER. The maximum correlation R= 0.9 is found at TAM and TSU station. Both TAM and TSU stations have SC events centered around the diagonal line and their slopes approach unity, in contrast to the HER station that has a lower slope and lower correlation coefficient. The large correlation at these two stations may result from their closer location to the average latitude of the Dst index stations. The low correlation at AAE station may be interpreted in terms of the enhanced noontime SC field as indicated by red dots, because noontime events show large variations with respect to the SYMH index, while at other stations the noontime events have homogenous variations similar to whole other local times. This equatorial noontime enhancement was noted by Ferraro and Unthank as mentioned earlier.

For the modelled field the correlation coefficient approaches R= 0.99 at all stations, with the slope of linear relationship increasing with approach to the magnetic equator. It reaches its maximum value $\frac{\Delta B_X}{\Delta SYMH}$ = 0.9 at AAE station while PEG and HER have the smallest slope $\frac{\Delta B_X}{\Delta SYMH}$ =0.73. TAM and TSU stations have comparable slopes $\frac{\Delta B_X}{\Delta SYMH}$ equal 0.82 and 0.84 respectively. The linear relationship between the modelled CM4 ΔB_X and $\Delta SYMH$ supports the claims of Sabaka et al (2004) that CM4 represents the horizontal magnetic field during active conditions up to 200-300 nT. The modelled results are expected because the model is parameterized using the Dst index; therefore a high correlation can be expected. However, despite the high correlation of the modelled ΔB_X field with respect to the $\Delta SYMH$ index, the points fall below the diagonal line, so CM4 under-estimates the $\Delta SYMH$ variations even at the equatorial station (AAE).

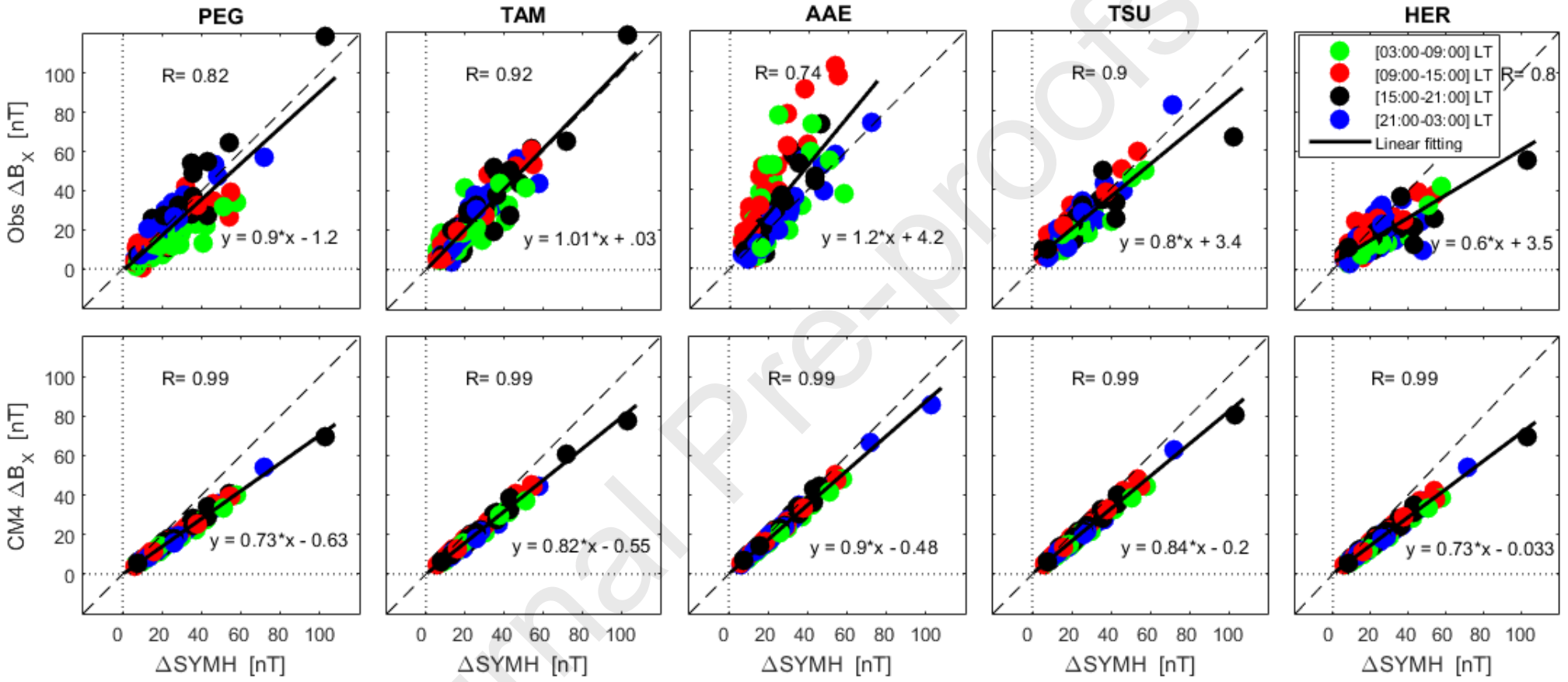

Fig. 8 The relationship between the observed ΔB_X field (upper panels) and the corresponding modelled CM4 ΔB_X field (lower panels) with $\Delta SYMH$ for the 5 INTERMAGNET observatories.Green, red, black and solid dots correspond to dawn, noon, dusk and night LTs, while the black solid and dashed lines represent the linear fit and 1:1 correlation respectively.

Discussion

The statistical analysis of SCs presented confirms that the modelled CM4 ΔB_X varies linearly with the $\Delta SYMH$ field irrespective of universal time in agreement with Sabaka et al. (2004). Fig. 6 showed that the modelled field only resembles the observed field at regions near $\pm 20^o$ magnetic latitudes. This include regions where the Dst index stations are located, but closer to the equator, the EEJ current strongly enhances the observed field variations during SCs. Therefore, this study provides evidence for locations where the CM4 gives a probable estimation of the external magnetospheric field during SCs.

Figure 8 shows that the relationship between the observed ΔB_X and $\Delta SYMH$ fields is scattered around the linear fitting line, in contrast to the modelled CM4 ΔB_X field that is well fit. Regardless, the slope of the modelled field increases with approach to the equator and becomes maximum - but less than 1 - at the equatorial station AAE. CM4 underestimates the $\Delta SYMH$ index, because CM4 model is parameterised by the Dst index for predicting the external magnetospheric fields. It also confirms the linearity between the CM4 ΔB_X and the $\Delta SYMH$ noted by Sabaka et al., (2004). However, the slopes of the observed field increase with approaching the equator; the correlation is maximum at TAM and TSU stations and minimum at AAE equatorial station. This establishes latitudinal limits for estimating the external magnetospheric field using the CM4 model. According to these results, the linearity in predicting the external magnetospheric field with respect to the D_{st} index which claimed by Sabaka et al., 2004 is only valid within the latitudinal location of the Dst or the SYMH stations.

However, CM4 gives a probable estimation of the external magnetospheric field at PEG and HER stations with respect to LT, although the seasonal variation of the observed field at northern and southern hemispheres does not appear in the modelled CM4 field. Figures. 9a-d compare the observed field at PEG and HER stations with their corresponding modelled CM4 field. It shows that the observed summer magnetospheric ΔB_X field strength at PEG is larger than the winter field strength, and vice versa at HER stations. This seasonal variation is not modelled in CM4, because the Dst index is derived from four stations located in northern and southern hemispheres, and the hourly value of the Dst index is the average magnetic field variations at these observatories. In addition, however, the observed field resembles the CM4 modelled field in its variation with respect to local time (minimum in the

early morning and maximum in the afternoon) except at the station close to the magnetic equator, it is broadly scattered in comparison to the modelled filed which has a very smooth narrow variations with respect to local time.

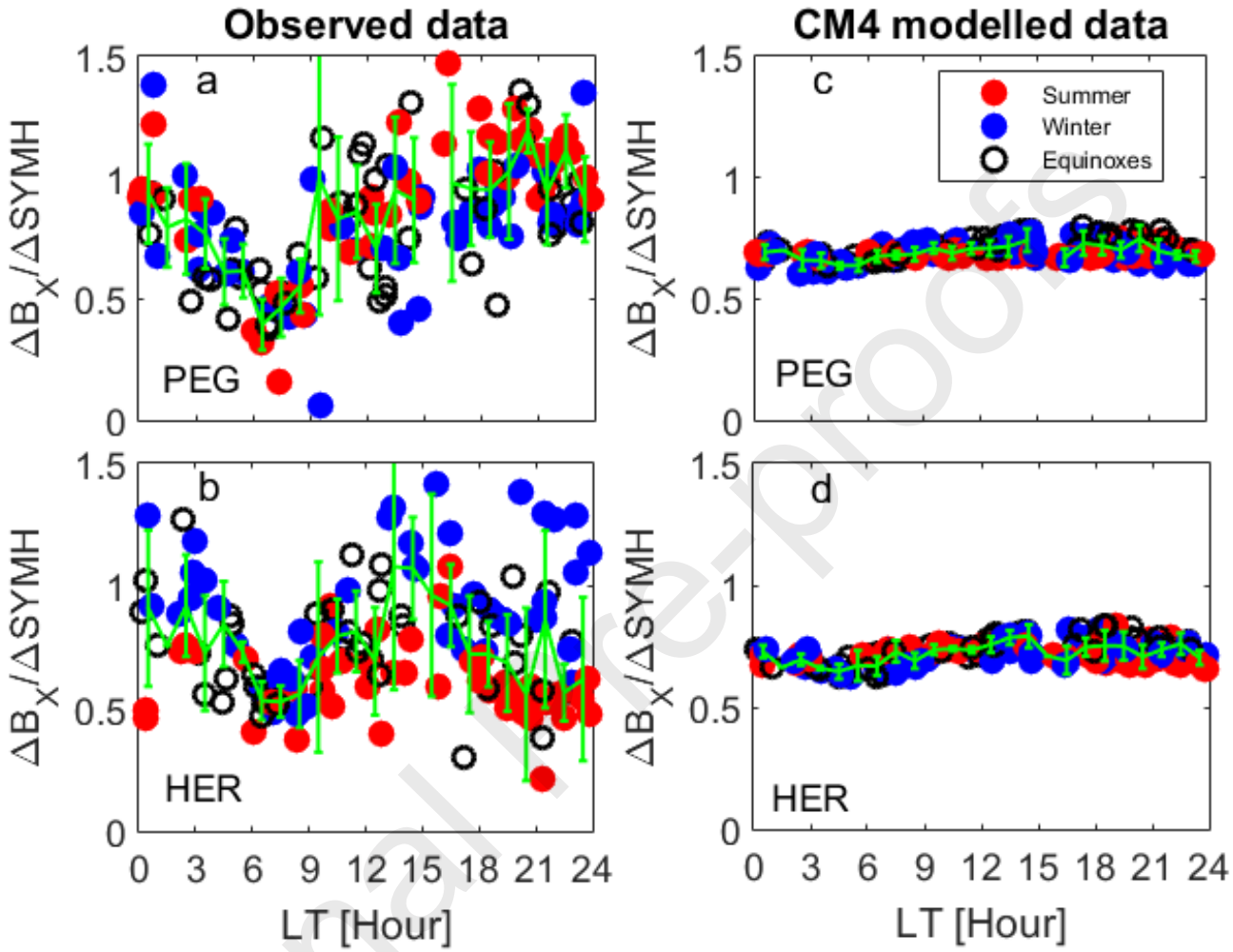

Fig. 9. (a-b) Variation of the normalized observed field with respect to LT at PEG and HER respectively and (c-d) Variation of the combined modelled magnetospheric CM4 field with respect to LT at PEG and HER. Blue, red and open black circles correspond to winter, summer and spring/autumn seasons respectively.

Not only are SC events observed at PEG, TAM and TSU are centered around diagonal lines, but they are also well-correlated with the SYMH index. Contrary to our expectation, most events observed at HER station are located under the diagonal line in contrast with AAE where most events are located above the diagonal line. Also, TAM and TSU stations have no broad scattered points and the slope $\left|\frac{\Delta B_X}{\Delta SYMH}\right|$~1 as shown in Fig. 10.

TAM and TSU are located at geomagnetic latitudes $+24.8^{o}$ and -18.7^{o} respectively, which is closer to the average latitude of Dst ground stations located within 22^{o} Suguira (1964). So, their observed ΔB_X field variations are better fit by $\Delta SYMH$ i than for stations at other latitudes. The slope of the observed field is larger than the modelled field at TAM because the SYMH field represents the average of the field recorded from 4 ground stations located at different local times.

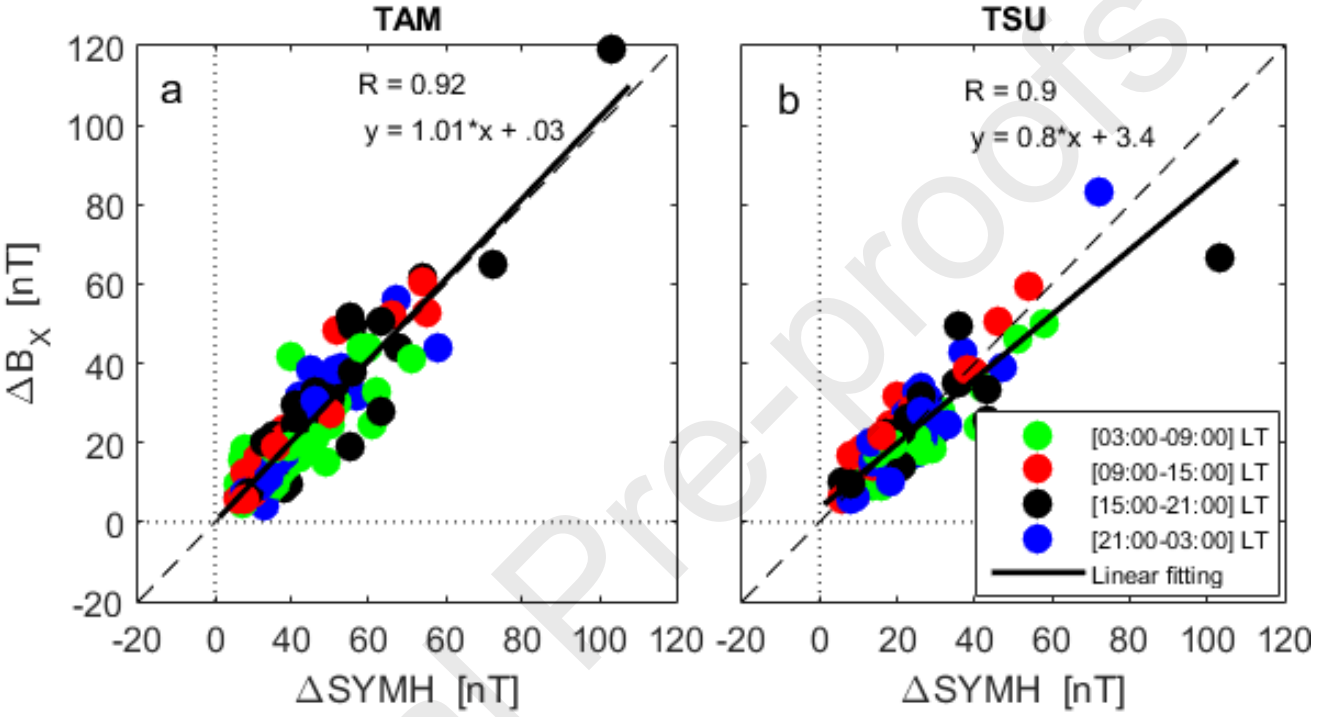

Fig. 10 The linear relationship between the observed ΔB_X and the $\Delta SYMH$ field strength, at a) TAM station and b) TSU station.

The SYMH index has magnetic effects from the RC, partial ring current (PRC), CFC, FAC and TC. Among these currents, only the CFC and the FAC systems have positive magnetic effects at the Earth's surface. Results show that even stations located farther from the magnetic equator have positive after-noon and nighttime enhancement for both modelled and observed data, which means that, consistent with SYMH index is not being a pure representation of the axial RC, but also with a significant contribution from the CFC and FACs as shown in Fig. 7. These results agree with Araki et al., (1994 and 2006) and Shinbori et al., (2009), who stated that $\Delta SYMH$ associated to SC is mainly caused by the CFC in the dayside and by the FACs in the nightside that are also modelled in the CM4 model.

Conclusion

This work investigates the possibility of using the comprehensive model (CM4) to predict variations of the external magnetospheric fields at days away from quiet times during geomagnetic SCs. The local time and seasonal dependences of SCs observed from five ground-based stations are compared with the modelled SC fields using the CM4 model. The study reflects the degree of consistency between ground observations and the CM4 modelled field during SCs at different latitudes.

The CM4 model shows that the maximum SC external magnetospheric field is located at the magnetic equator and decreases gradually towards the poles. The relationship between the CM4 $\frac{\Delta B_X}{\Delta SYMH}$ field and LT showed maximum field variations in the afternoon and the minimum variations in the early morning which is a signal of the PRC. These local-time features exist at all latitudes inside the model and coincide with the observed features.

The linear relationship between the observed field ΔB_X and the variation in the $\Delta SYMH$ index at the equatorial station (AAE) has the largest slope 1.2, and smallest correlation coefficient 0.74 and the whole dayside SC events are located over the diagonal line. The reason for that is the high contribution of the EEJ current to the observed field. HER station has the smallest slope 0.6, and most points are located below the diagonal line in comparison with TAM and TSU stations that have the highest correlation and the whole events are centered around the diagonal line. The relationship between the observed field $\frac{\Delta B_X}{\Delta SYMH}$ and LT showed seasonal variations between summer and winter seasons. The $\frac{\Delta B_X}{\Delta SYMH}$ field is larger in summer than in winter in the northern hemisphere at PEG station, while in the southern hemisphere it is smaller in summer than in winter at HER station. This seasonal variation is not modelled by the CM4 model because it is parameterized by the Dst index, which is derived from ground stations located in both hemispheres and also at different local times.

However, the CM4 model successfully predicts the SC variations as they vary in a linear form with respect to variations in the $SYMH$ index, cautions should be considered at equatorial stations or stations located away from the average latitude of the Dst index stations. In addition, the strength of the observed fields differ from the modelled field, even at the latitude of the Dst index stations. Again, the CM4 has no information about the seasonal field variation during summer and winter in both hemispheres.

Acknowledgements

Authors, would like to thank the institutes of PEG, TAM, AAE, TSU and HER observatories for supporting their operation and extend their great thanks to INTERMAGNET for promoting high standards of magnetic observatory practice (www.intermagnet.org). This work funded by Egyptian cultural bureau for pursuing a postdoctoral study at the School of Environment and Oceanography–Liverpool University, UK. The authors thank two anonymous reviewers for their fruitful discussion and comments.

References

Araki, T. (1994), A physical model of the geomagnetic sudden commencement, in Solar Wind Sources of Magnetospheric Ultra-Low-Frequency Waves, Geophys. Monogr. Ser., vol. 81, edited by M. J. Engebretson, K. Takahashi, and M. Scholer, p. 183, AGU, Washington, D.C.

Araki, T., T. Takeuchi, and Y. Araki (2004), Rise time of geomagnetic sudden commencements—Statistical analysis of ground geomagnetic data, Earth Planets Space, 56, 289.

Araki, T., K. Keika, T. Kamei, H. Yang, and S. Alex (2006), Nighttime enhancement of the amplitude of geomagnetic sudden commencements and its dependence on IMF-Bz, Earth Planets Space, 58, 45– 50.

Barkhatov N.A. Levitin A.E. Tserkovnyuk O.M. Relation of the Indices Characterizing the Symmetric (SYM) and Asymmetric (ASY) Ring Currents to the AE (AU, AL) Indices of Auroral Electrojet Activity, Geomagnetizm and Aeronomiya, 48, 520, 2008.

Burton R.K. McPherron R.L and Russell C.T., (1975), An empirical relationship between interplanetary conditions and Dst, J. Geophys. Res, 80, 4214.

Fathy, A., Kim, K.-H., Park, J.-S., Jin, H., Kletzing, C., Wygant, J. R., & Ghamry, E. (2018). Characteristics of sudden commencements observed by Van Allen Probes in the inner magnetosphere. Journal of Geophysical Research: Space Physics, 123, 1295–1304. https://doi.org/10.1002/2017JA024770

Ferraro, V. C. A., and H. W. Unthank (1951), Sudden commencements and sudden impulses in geomagnetism: Their diurnal variation in amplitude, Geofis. Pure Appl., 20, 27– 30.

Iymori T. (1990), Storm-time magnetospheric currents inferred from mid-latitude geomagnetic field variations, J. Geomag. Geoelectr. 42, 1249.

Walker J. S.(2008). A primer on wavelets and their scientific applications. 2nd ed.

Kalegaev V.V. Ganushkina N.Y. Pulkkinen T. Tsyganenko N.A. Friedel R.H.W. (Eds.) (2005), Physics and Modeling of the Inner Magnetosphere, AGU Geophysical Monograph 155. AGU, Washington, DC, p. 293.

Kalegaev V.V. Makarenkov E.V (2008), Relative importance of ring and tail currents to Dst under extremely disturbed conditions. Atmo.Terr.Phys, 70, 519-525.

Kamide Y (2000), From discovery to prediction of magnetospheric processes; Journal of Atmospheric and Solar-Terrestrial Physics.62, 1668.

Langel, R.A., and R.H. Estes (1985a), Large-scale, near-Earth magnetic fields from external sources and the corresponding induced internal fields, Journal of Geophysical Research, 90, 2487-2494.

Li, H., C. Wang, and J. R. Kan (2011), Contribution of the partial ring current to the SYMH index during magnetic storms, J. Geophys. Res., 116, A11222, doi:10.1029/2011JA016886.

Mcpherron R. L (1999), Influence of substorm current wedge on Dst index, J.Geophys.Res. 104, 4567-4575.

Menvielle M and Marchaudon A (2007). Geomagnetic indices in solar terrestrial physics and space weather, 277-288.

Onovughe, E. and Holme, R. (2015), The CM4 model prediction of ground variation of the geomagnetic diurnal field away from quiet time, Physics of the Earth and Planetary Interiors 249, 1–10.

Onovughe, E. (2016), Can the comprehensive model phase 4 (CM4) predict the geomagnetic diurnal field for days away from quiet time? Ann. Geophys., 34, 887–900, doi:10.5194/angeo-34-887.

Park, J.-S., Kim, K.-H., Lee, D.-H., Araki, T., Lee, E., & Jin, H. (2012). Statistical analysis of SC-associated geosynchronous magnetic field perturbations. Journal of Geophysical Research, 117, A09212. https://doi.org/10.1029/2012JA017648

Park, J.-S., Kim, K.-H., Kwon, H.-J., Lee, E., Lee, D.-H., Jin, H., & Hwang, J. (2014). Statistical analysis of geosynchronous magnetic field perturbations near midnight during sudden commencements. Journal of Geophysical Research: Space Physics, 119, 4668–4680, https://doi.org/10.1002/2013JA019380.

Rawat R., Alex S., Lakhina G.S. (2010) Storm time time characteristics of of intense geomagnetic storm (Dst≤-200 nT) at low latitude and and associated energetic, Atmos. Terr. Phys, 72, 1371, https://doi.org/10.1016/j.jastp.2010.09.029

Sabaka, T. J. and Baldwin, R. T. (1993), Modeling the Sq magnetic field from POGO and MAGSAT satellite and cotemporaneous hourly observatory data: Phase 1, Technical Report Contract Report HSTX/G&G9302, Hughes STX Corp., for NASA/GSFC Con-tract NAS5-31 760, NASA.

Sabaka, T. J., N. Olsen, and R. A. Langel (2002), A comprehensive model of the quiet-time near-Earth magnetic field: phase 3. Geophysical Journal International, 151, 32-68.

Sabaka, T.J, N. Olsen and M.E. Purucker (2004). Extending Comprehensive models of the Earth's magnetic field with Oersted and CHAMP data. Geophysical Journal International, 159, 521-547.

Sugiura M., 1964, Hourly values of equatorial Dst for IGY., 35, 948.

Shinbori, A., T. Ono, M. Iizima, and A. Kumamoto (2004), SC related electric and magnetic field phenomena observed by the Akebono satellite inside the plasmasphere,Earth Planets Space, 56, 269–282.

Shinbori, A, T. Ono, M. Iizima, A. Kumamoto, Y. Nishimura (2006) Enhancements of magnetospheric convection electric field associated with sudden commencements in the inner magnetosphere and plasmasphere regions Advances in Space Research 38 1595–1607

Shinbori, A., Yuji Tsuji, Takashi Kikuchi, Tohru Araki, and Shinichi Watari (2009), Magnetic latitude and local time dependence of the amplitude of geomagnetic sudden commencements, JGR, 114, A04217, doi:10.1029/2008JA013871

Turner N. E., Baker D. N., Pulkkinen T. I., and McPherron R. L (2000), Evaluation of the Tail Current Contribution to Dst, J. Geophys. Res., 105, 5431.

Declaration of interests

☒ The authors declare that they have no known competing financial interests or personal relationships that could have appeared to influence the work reported in this paper.

☐The authors declare the following financial interests/personal relationships which may be considered as potential competing interests:

Dr. Adel Fathy Abdelmoneam
Fayoum University, Physics Department, Faculty of Science, Egypt
Email: afa05@fayoum.edu.eg